Intermolecular Interactions and their Implications in Solid-State Photon Interconversion

Lea Nienhaus*

Abstract: Photon interconversion promises to alleviate thermalization losses for high energy photons and facilitates utilization of sub-bandgap photons – effectively enabling the optimal use of the entire solar spectrum. However, for solid-state device applications, the impact of intermolecular interactions on the energetic landscape underlying singlet fission and triplet-triplet annihilation upconversion cannot be neglected. In the following, the implications of molecular arrangement, intermolecular coupling strength and molecular orientation on the respective processes of solid-state singlet fission and triplet-triplet annihilation are discussed.

Keywords: Aggregation · Intermolecular coupling · Singlet fission · Triplet-triplet annihilation

Dr. Lea Nienhaus obtained her BSc in Chemistry from the Universität Ulm in 2010 and her PhD from UIUC in 2015. After her postdoctoral work at MIT, she began her independent career as an Assistant Professor at Florida State University in 2018. In 2024, she moved to Rice University as an Associate Professor. The group has pioneered solid-state perovskite-sensitized photon upconversion using a variety of tetracene and anthracene derivatives. The Nienhaus Research Group is interested in understanding the role of nanoscale structure on ensemble materials properties. The utilized combination of optical spectroscopy and scanning probe microscopy enables a unique understanding of the complex photophysical processes occurring in these systems.

1. Introduction

Photon interconversion is a promising approach to increase the achievable solar cell efficiency and increase the device longevity due to filtering of high-energy photons. Photon downconversion *via* singlet fission (SF) in polyaromatic hydrocarbons (PAHs) promises to alleviate thermalization losses by converting one high energy photon into two spin-triplet states, which, once transferred into a photovoltaic device (PV) can produce two electrons and two holes which can be extracted as current.[1–4] Photon upconversion (UC) *via* triplet-triplet annihilation (TTA) on the other hand can be utilized to convert sub-bandgap photons – that otherwise cannot be used to generate current in a PV – to higher energy photons which in turn can be absorbed by the PV.[5,6] Hence, by expanding the portion of the solar spectrum that can be used and by more efficiently utilizing the high-energy portion of the spectrum, the device performance can be enhanced.

Beyond possible applications in PVs,[7] upconversion bears promise for applications including photocatalysis,[8] bioimaging[9] and anticounterfeiting.[10]

First invoked in 1965 to understand the photophysical properties of anthracene,[11] the field of SF has greatly expanded over the years, with both time-resolved spectroscopy and magnetic field-dependent studies providing the necessary window into the ongoing processes.[12–16] Dexter first proposed utilizing the triplet excitons generated by SF to sensitize silicon photovoltaics in 1979,[2] an idea which took several more decades to be realized due to the sensitive nature of the silicon surface.[1,17–20] On the other hand, triplet exciton energy transfer (TET) into semiconductor quantum dots was successful quickly and sparked a new direction in the field of sensitized UC.[21]

TTA-UC was first observed in anthracene in 1962 by Parker and Hatchard.[22] Since then, sensitized TTA-UC has emerged as an independent research direction, based on the seminal work by Castellano and co-workers in the early 2000s.[23–27] Most of the work since then has focused on understanding the photophysics of both triplet energy transfer process between the sensitizer and annihilator and the TTA-UC process itself.[28–40] Beyond conventional metal-organic complexes which generate triplet states through intersystem crossing,[26] additional triplet sensitization mechanisms based on inorganic/organic hybrid systems have been explored. Semiconductor nanocrystals for example, have an exchange energy gap between the singlet and triplet state on the order of ambient thermal energy $k_B T$.[41] As a result of strong spin-orbit coupling in semiconductor quantum dots, spin is not the good quantum number, rather the total angular momentum is relevant.[41] Due to this strong spin-mixing, the lowest energy exciton wavefunction contains both a singlet and a triplet-related term, and the exciton can therefore couple directly to the triplet state of an annihilator without an additional intersystem crossing step.[30,32,42] Beyond excitonic triplet sensitizers, it is also possible to generate bound triplet excitons by charge injection, followed by subsequent recombination to form the triplet state.[33,34,43–45]

In the following, we will briefly introduce the mechanisms of SF and TTA-UC and discuss how intermolecular interactions in PAHs in the solid-state impact each process. This review is not intended to be all-encompassing, rather it is meant to specifically highlight the possible impact of intermolecular coupling on SF and TTA-UC. For a deeper dive into the fields of SF and TTA-UC, we refer the interested reader to additional existing review articles.[5,6,46–50] An overview schematic of SF and TTA-UC is shown

Correspondence: Dr. L. Nienhaus, E-mail: nienhaus@rice.edu, Dept. of Chemistry, Dept. of Physics and Astronomy, Dept. of Materials Science and Nanoengineering, Rice Advanced Materials Institute, Rice University, Houston, Texas 77005, USA
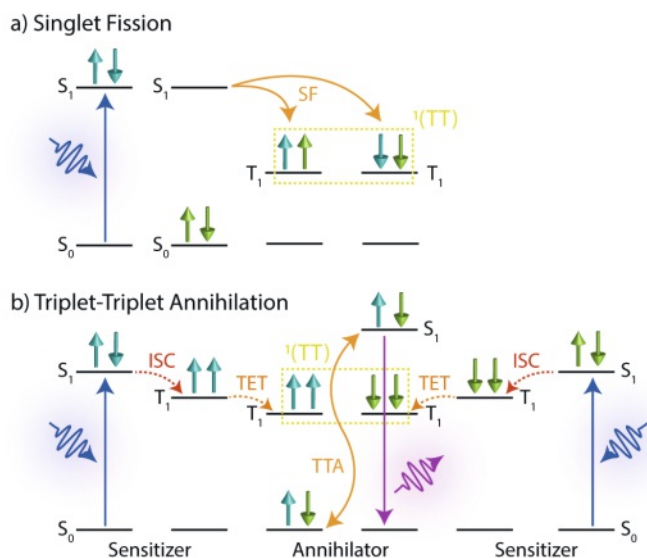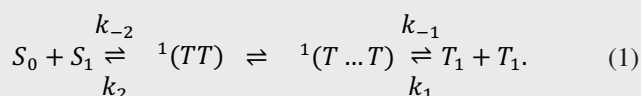
Fig. 1. Schematic of the mechanism of a) singlet fission (SF) and b) conventional molecular sensitized triplet-triplet annihilation (TTA). Upon excitation of the singlet state, the sensitizer undergoes intersystem crossing (ISC) to the triplet state, which then can be transfered directly to the annihilator in a spin-allowed Dexter-type triplet energy transfer mechanism (TET). The formal electron exchange and spin states are included to highlight that both processes are overall spin-allowed.

in Fig. 1, where SF generates two triplet states in a spin-allowed process. In the TTA-UC process, triplet states in the sensitizer are initially generated by intersystem crossing (ISC) followed by triplet exciton transfer (TET) to the annihilator and subsequent bimolecular TTA-UC.

1.1 *Singlet Fission*

In SF, an organic chromophore in the spin-singlet excited state interacts with a neighboring chromophore in its ground state. By sharing the excited state energy, both chromophores convert to spin-triplet states in a spin-allowed process. Generally, the SF process is described by the following simplified kinetic scheme:[46]

$$S_0 + S_1 \underset{k_2}{\overset{k_{-2}}{\rightleftharpoons}} {}^1(TT) \rightleftharpoons {}^1(T \dots T) \underset{k_1}{\overset{k_{-1}}{\rightleftharpoons}} T_1 + T_1. \tag{1}$$

The correlated triplet pair state $^1(TT)$ is formed from the initial singlet excited and ground state with rate k_{-2} and can reform the ground and excited singlet states with rate k_2. As the triplet states begin to diffuse to non-neighboring molecules the spatially separated $^1(T\dots T)$ state is formed, which still exhibits overall spin-singlet character. In the final step the separated $^1(T\dots T)$ subsequently spin-relaxes into two uncorrelated triplet states with rate k_{-1}.[3,46,51] Additional relaxation pathways involving the spin-triplet and quintet triplet pair states [$^5(TT)$ and $^3(TT)$] are in principle possible, however, will not be discussed here but can be found elsewhere.[52–55]

The rate k_{-2} can be expressed as an Arrhenius-type equation based on the average nuclear deformation energy between the states S_1 and T_1, the average frequency of molecular vibrations $\langle\omega\rangle$, the energy difference ΔE between the singlet state S_1 and correlated triplet pair state $^1(TT)$ and the average exchange interaction matrix element V:[46]

$$k_{-2} = \frac{6\pi^{\frac{1}{2}}|V|^2}{\hbar(2\hbar\langle\omega\rangle E')^{\frac{1}{2}}} \exp\left[-\frac{(\Delta E - E')^2}{4\hbar\langle\omega\rangle E'}\right], \tag{2}$$

A fundamental requirement of the feasibility of this process is that the triplet state energy $E(T_1)$ is equal or less than half of the singlet energy $E(S_1)$, although entropic effects can lead to successful SF in slightly endothermic systems:[6]

$$E(S_1) \geq 2E(T_1). \tag{3}$$

Anthracene was the first molecule in which SF was invoked to fully understand the photophysical processes.[11] Since then, a wide range of singlet fission materials have been found, including polyacenes such as tetracene and pentacene,[56–60] carotenoids[61,62] and conjugated polymers such as diacetylenes and thiophenes.[63,64]

1.2 *Triplet-Triplet Annihilation*

TTA describes the opposite process of SF: the formation of a spin-singlet state and a ground state from two triplet states. In the simplest case, TTA-UC can be approximated by the following kinetic scheme:

$$T_1 + T_1 \underset{k_{-3}}{\overset{k_3}{\rightleftharpoons}} S_1 + S_0, \tag{4}$$
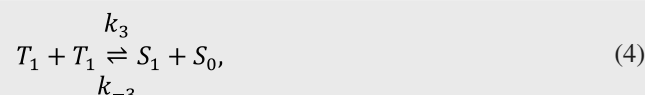
a more detailed description would be the reverse reaction of Eqn. (1). Here, the rate k_3 describes the rate of singlet generation, while the reverse rate k_{-3} would correspond to the reverse process of singlet fission. Again, the rate of TTA is dependent on the strength of the exchange coupling between the two initial triplet states:

$$k_3 \propto |V_{exchange}|^2. \tag{5}$$

To comply with energy conservation laws, here, twice the triplet energy must be equal or more than the singlet energy:[6]

$$E(S_1) \leq 2E(T_1). \tag{6}$$

If the energy levels of the triplet and singlet state align such that the singlet energy is within several $k_B T$ of twice the triplet energy, both SF and TTA can occur – leading to a competition between the processes, where the individual rates become critical to predict which process will dominate.

1.3 *Brief Overview of the State of the Field*

SF has been observed in highly concentrated solutions, in solid films, in single crystals, and in isolated dimers.[60,65,66] In solution, the mechanism is still under debate. The required interaction between chromophores has been proposed to be either diffusion-mediated or aggregation-mediated.[65,67,68] In solid films on the other hand, different intermolecular coupling based on the local crystal structure can result in changing rates of SF. Generally, the ordered nature of crystalline films and single crystals primes these morphologies for fast and efficient SF.[69–71] In amorphous films, SF has been observed for some materials,[72] even enhanced over their crystalline counterparts.[73] On the other hand, suppression of SF has been observed in amorphous rubrene.[74,75] Overall, a clear predictive correlation between the local crystal structure/molecu-

lar arrangement and the success of SF is still lacking, however, efforts are being made to fill this gap. One approach which is being pursued is the synthetic fabrication of dimers capable of SF, where the orientation and separation of the individual chromophore units is dictated by the linker used.[76–80]

TTA-UC on the other hand has been primarily successful in solution phase at moderate concentrations to avoid inner filtering effects and reabsorption.[24,32,81–85] Several attempts have been made to translate the relatively high efficiencies obtained in solution into the solid state using polymer or gel matrices.[27,86–89] While upconversion is observed, the upconversion yields are significantly lower than in solution, which is in large part due to a lowered triplet collision rate based on the reduction of diffusion.

Hybrid organic/inorganic solid-state devices consisting of bilayers of the sensitizer and triplet annihilator bear great promise for applications in solar energy, however, have to date also not returned the expected efficiencies. PbS quantum dot-based bilayer upconversion devices have faltered due to limited exciton diffusion in the PbS layer limiting the achievable absorption.[90] While lead halide perovskite-based upconversion devices have overcome the limited absorption of the PbS quantum dots, the required charge extraction of both electron and hole at the same interface has proven to be a limiting factor in the number of triplet states that can be generated.[31,34]

True bilayer devices bear an additional challenge: intermolecular interactions in the molecular annihilator. Rubrene, to date the state-of-the-art triplet annihilator for solid-state upconversion devices, shows no ill effects with respect to its optical properties upon condensation into the solid-state in large part due to its phenyl side groups. However, other potential annihilators such as 1-chloro-9,10-bis(phenylethynyl)anthracene[91] and naphtho[2,3-a]pyrene[92] both show redshifted absorption features which can be attributed to J-type coupling,[93] leading to changes in the underlying energy landscape. These additional complications have, in part, led to diminished success of solid-state UC devices.

2. Issues in the Solid State: Aggregates, Excimers, Order & Disorder

Many PAHs show a change in their optical properties between the isolated molecule in a dilute solution and a more concentrated solution or in solid state, a result of intermolecular coupling influencing the allowed transitions. This is a particular issue in planar PAHs, which are primed for strong π-π stacking interactions.

Anthracene is known to photodimerize upon optical excitation,[94] but also forms excited state dimers or excimers in solution and solid state.[95,96] To in part overcome these issues, 9,10-diphenylanthracene, or DPA, was introduced as a similar triplet annihilator, as the dimerization process is blocked by the phenyl groups. However, DPA still suffers from excimer formation in solid films.[97,98] Rubrene on the other hand, has the benefit of four twisted phenyl groups, which adds steric hindrance to the prerequisite close packing for intermolecular coupling, facilitating the formation of more amorphous films.[74,75] In the following, the effects of intermolecular coupling on the optical properties will be introduced in detail, followed by a discussion on how these changes in the energy landscape influence SF and TTA.
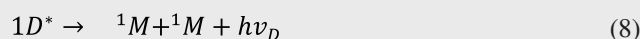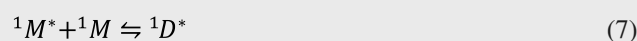
2.1 Intermolecular Coupling Effects

In addition to enhancement of non-radiative decay pathways to suppress emission or aggregation-induced enhancements of the emission, three distinct impacts of intermolecular coupling will be discussed here in detail: excimer formation, H- and J-type aggregation.[93,99–101]

Excimers are formed upon the interaction of an excited state molecule with a ground state molecule. Strictly speaking, an excimer consists of two of the same molecules, while an exciplex is a broader term encompassing an excimer state across two different molecule types. The excimer state describes the sharing of the excited state across two molecules and the exciton is delocalized across both molecules. Since the excimer only exists in the excited state, and the 'dimer' dissociates upon relaxation to the ground state, no steady-state absorption feature is associated with the excimer state. Excimer emission is lower in energy than the monomer emission and is generally broad and featureless due to its dissociative nature in the ground state.[99]

In addition, the excimer commonly relaxes with a slower rate and lower quantum yield than the monomer, leading excimer formation to be a self-quenching mechanism. Excimer formation can be summarized by the following kinetic model describing the excimer formation $^1D^*$ and its subsequent relaxation to two ground state monomers ^1M upon release of a photon.

$$^1M^* + {}^1M \leftrightharpoons {}^1D^* \tag{7}$$

$$1D^* \rightarrow \quad ^1M + {}^1M + h\nu_D \tag{8}$$

Aggregation on the other hand, leads to noticeable changes in both the ground and excited state properties, as intermolecular coupling influences the allowed optical transitions and oscillator strength. The effect of intermolecular couplings present during molecular aggregation on the resulting photophysical properties was first investigated by Kasha.[102–104] Within the point-dipole approximation limit, the Coulomb coupling V between the transition dipole moments $\vec{\mu}$ of two monomers can be described based on the angle θ between the dipole vectors and the center-to-center distance vector $\vec{R}$, while R is the magnitude of this vector between the point dipoles.

$$V = \frac{\mu^2(1-3\cos^2\theta)}{4\pi\varepsilon R^3} \tag{9}$$

Depending on whether this coupling term is positive or negative, H- or J-type aggregation is observed, respectively.[102–105] The magic angle is $\theta_m = 54.7°$. At angles θ smaller than θ_m, $V < 0$ and J-type coupling is observed, while larger angles result in $V > 0$ and H-type coupling is obtained. As a direct result of the sign of the coupling term V, the allowed absorption (in-phase transition) of J-aggregates is shifted to lower energies (red-shifted), while in H-aggregates, the allowed transition is shifted to higher energies (blue-shifted). The out-of-phase (disallowed) combination of the transition dipoles yields a higher energy state in J-aggregates and a lower energy state in H-aggregates. Since H-aggregates have an allowed optical transition into the high energy state denoted as *S"$_1$ in Fig. 2, rapid intraband relaxation can occur to the lowest lying (antisymmetric) state *S'$_1$, from which the radiative transition to the ground state is forbidden due to symmetry. Hence, due to very slow radiative transition rates, emission is commonly greatly suppressed in H-aggregates. In J-aggregates on the other hand, the (symmetric) lowest energy state can couple directly to the ground state. The rate of radiative recombination is enhanced by a factor of N, the number of coupled molecules. Hence, superradiance is commonly observed in J-aggregates.[93]

Strictly speaking, this classification is used for one-dimensional aggregates. Upon two- or three-dimensional aggregation present in solid crystals of PAHs, both H- and J-type couplings can be present. This leads to the typical HJ aggregates discussed by Spano and coworkers for PAHs in herringbone arrangements[93,106] or the I-aggregates coined by Caram and coworkers.[107,108]
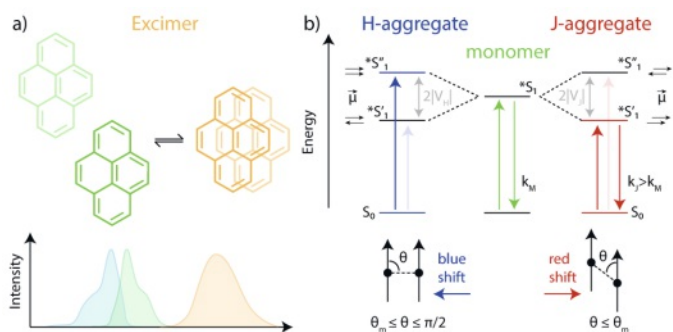
Fig. 2. a) Schematic of excimer formation and its impact on the emission spectrum (blue:monomer absorption, green: monomer emission, orange: excimer emission). b) Simplified energy level diagram for the H- and J-aggregate formation due to absolute value of the electronic coupling |V| between monomer units.

Considering the direct impact of intermolecular interaction on the resulting photophysical properties including the radiative recombination rates and emission wavelength, a clear impact on both SF and TTA-UC can be anticipated. Both the Coulomb interaction underlying the aggregation-related changes in the optical properties and the exchange interaction underlying SF and TTA are strongly related to the molecular arrangement and distance between chromophores, hence, it is expected that SF and TTA are correlated to the local molecular arrangement.[109] In J-aggregates, in the simplest case, the enhanced radiative rate could lead to a competition between the rate of SF and radiative emission.[110] Furthermore, J-type aggregation results in a lowering of the lowest energy singlet state, which in turn can result in energetically unfavored SF, as the lowest energy singlet state S_1 could be lowered below twice the triplet energy, thus making SF endothermic. However, the coupling V can similarly impact the rate of SF such that the rate of SF is diminished in H-aggregates and enhanced in J-aggregates.[110] Excimer formation on the other hand, could also yield a competing relaxation pathway and results in diminished SF returns.

For UC applications on the other hand, excimer formation can limit the achievable energy gain, the apparent anti-Stokes shift. However, strong coupling between two molecules may result in localized strongly TTA-active sites. In the following, we will give a short overview of the existing literature discussing the impact of molecular arrangement on SF and TTA-UC.

3. Impact of Coupling Strength on SF

It is clear that the intermolecular coupling dictated by the molecular level arrangement is an important parameter for successful SF. However, it is not the only critical factor. A theoretical study by Yost et al.[111] established a model to predict SF kinetics. In the weak coupling limit, the SF rate k_{SF} follows a Marcus-type[112,113] non-adiabatic relationship:

$$k_{SF} \approx \frac{2\pi}{\hbar} \bar{V}^2 \frac{1}{\sqrt{4\pi\lambda k_B T}} e^{-\frac{(\Delta G + \lambda)^2}{4\lambda k_B T}} \qquad (10)$$

where the SF from the coupled $S_1 S_0$ state occurs suddenly to form the ^{1}(TT) state and the rate of SF is directly proportional to $\bar{V}^2$. On the other hand, in the strong coupling limit, SF tracks the adiabatic state, and the ^{1}(TT) state will be gradually generated from $S_1 S_0$ (Fig. 3). Here, the rate of SF becomes independent of the coupling strength $\bar{V}$ and is instead related to the timescale of nuclear rearrangement τ_{ad}. The overall SF rate as a function of coupling strength is well described by the rate expression by Bixon and Jortner:[114]

$$k_{SF} = \sum_n \frac{\overline{V^2} k_n}{1 + \tau_{ad,n} \overline{V^2}} \qquad (11)$$

where the rate is limited by the non-adiabatic rate k_n (proportional to ΔG) for weak coupling and by the adiabatic timescale τ_{ad} for strong coupling. Hence, while the coupling strength is important, to first approximation, exergonic SF ($\Delta G < 0$) is the most critical factor for high SF rates. Simply increasing the intermolecular coupling eventually results in a plateau of the SF rate due to the transition into the adiabatic regime, with no further benefit.[111] Maintaining exothermic SF, i.e. $E(S_1) > 2 \times E(T_1)$ is therefore the most important aspect for obtaining high rates of SF.[115] However, care must be taken to remain within the Marcus normal region.[116]
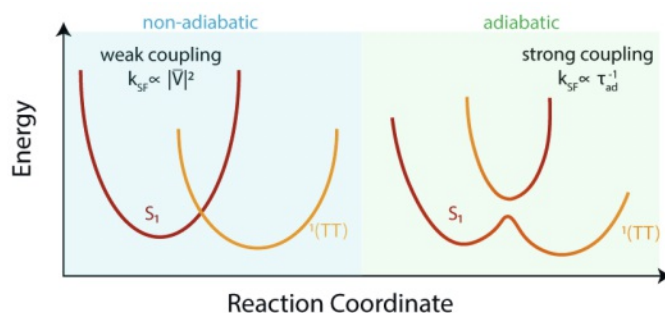

Fig. 3. Schematic of the energy landscape of SF for the weak coupling (non-adiabatic) and strong coupling (adiabatic) case.

3.1 Role of Order and Disorder

Beyond simple coupling strength, the coupling term is also sensitive to the orientation of the molecules in the solid. Hence, to first approximation, long-range ordered crystal structures are primed to yield high SF yields.

In disordered films where there is a lack of long-range coupling, suppression of SF has been observed.[117,118] For example, in amorphous rubrene film, the absence of SF has been reported.[74] As a result, vapor-deposited (polycrystalline) rubrene films require an additional dopant dye to suppress fluorescence quenching effects caused by SF,[30,119] while spin-coated (amorphous) rubrene thin films do not show a noticeable enhancement in quantum yield upon doping.[75]

To elucidate the SF properties of a disordered thin film, Roberts et al. investigated SF in 5,12-diphenyl tetracene (DPT) thin films.[73] In contrast to the parent molecule tetracene, which forms an ordered herringbone-type crystal structure during vapor deposition, the additional phenyl groups in DPT frustrates ordered crystal growth, resulting in amorphous films without greatly impacting the singlet and triplet energy manifold. In contrast to thin films of tetracene which exhibit effects caused by J-type coupling and splitting of the vibronic progression due to Davydov coupling,[120] the vapor-deposited thin film of DPT shows absorption and emission features which are very similar to the respective features of isolated DPT molecules in solution. This is a clear indication that no strong coupling is present between individual DPT molecules in the thin film and that the singlet state is localized on a single molecule.[73]

A SF yield of 61% is reported and half of the triplets are initially formed on a ~1ps timescale, followed by slower formation of the remaining triplet states within the first 100 ps. Hence, the authors conclude that there are localized hotspots of SF, where the local cofacial arrangement of DPT molecules results in favorable SF (Fig. 4).[121] Rapid SF occurs for singlet states near the hotspot, while the slower timescale corresponds to triplet states generated

after singlet diffusion to the SF hotspot.[73] The molecular arrangement of the SF hotspots was further investigated in detail by density functional theory (DFT) simulations by Mou *et al.*[121] who determined two dimer arrangements with a twist or slide stacking arrangement which resulted in high SF rates.
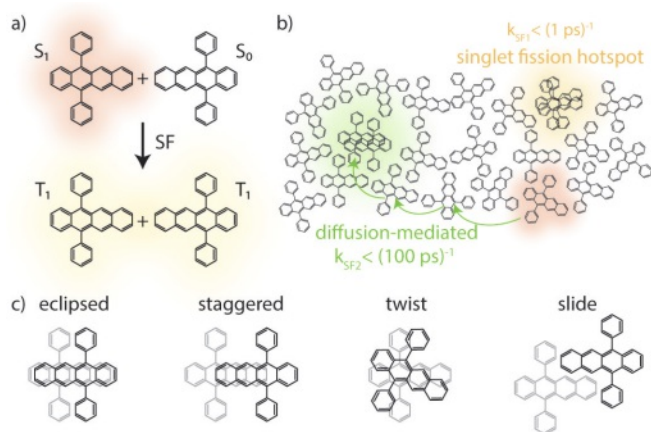

Fig. 4. a) SF in DPT forming two spin-triplet states from an excited spin-singlet state S$_1$ and a singlet ground state S$_0$. b) Cartoon highlighting the two different SF mechanisms resulting in the two timescales: rapid SF at local hotspots and diffusion-mediated SF. c) Schematic of the DPT molecular arrangement in a crystal (eclipsed and staggered) and the SF dimers determined to have the highest rate of SF.

Similarly, Volek *et al.* recently reported that SF was enhanced at the border of disordered regions at the edges of rubrene crystals.[122] The spatial orientation of the molecules dictates the HOMO-LUMO overlap. Rubrene is a unique case of a SF material, where the HOMO-LUMO spatial overlap is zero in the orthorhombic crystal structure based on symmetry. Hence, in a completely ordered rubrene crystal in absence of any vibrational movement that break symmetry, SF is a forbidden process.[123]

In agreement with previous reports,[74] the work by Volek *et al.* indicates negligible coupling in fully amorphous regions of rubrene leading to diminished SF, while vibrational symmetry breaking facilitates SF in the crystal.[122] However, SF hotspots are found at regions between the ordered crystal and amorphous regions. This region at the border of order and disorder is able to retain a high degree of structural order, however, local rubrene dimers have sufficient disorder to break symmetry and allow for enhanced SF rates.

On the other hand, Pensack *et al.* investigated the impact of the crystallinity on the SF dynamics of 6,13-bis(triisopropylsilylethynyl)pentacene (TIPS-Pn) nanoparticles showing the importance of ordered molecular arrangement for SF in TIPS-Pn.[124] Rapid and lossless SF is observed in crystalline TIPS-Pn nanoparticles on a timescale of ~ 100 fs, resulting in two triplets formed per excited singlet state. In amorphous nanoparticles on the other hand, only 1.4 triplets are formed per excited singlet state, indicating significant loss channels. Here, the excited state population decays rapidly prior to triplet pair separation. Importantly, no migration between amorphous and crystalline regions is observed, indicating that the existing loss channels in amorphous regions cannot be mitigated by energy funneling to nearby lower-energy crystalline regions.[124]

Even different crystalline environments can result in different SF rates due to a change in the intermolecular coupling. Many PAHs exhibit polymorphism, hence, they can adopt several crystal structures in solid state based on the crystallization conditions. Beyond the simple consideration of the SF molecule, here, the polymorph must also be considered. For example, in 9,10-bis(phenylethynyl) anthracene the rate of singlet fission changes between the *Pbcn* and *C2/c* polymorphs, where the π-π stacking distances are 3.45 and 3.40 Å, with a longitudinal slip of 3.34 and 4.06 Å, respectively (Fig. 5).[66] These morphological differences significantly influence the intermolecular interactions resulting in SF rates of $k_{C2/c}$ = (109±4 ps)$^{-1}$ and k_{Pbcn} = (490±10 ps)$^{-1}$.[66]

Overall, a clear overarching prediction whether an ordered crystalline structure or a disordered material is beneficial for SF is difficult to make. As demonstrated with the examples discussed here, there are several aspects that must be taken into consideration and each SF molecule exhibits distinct behavior.
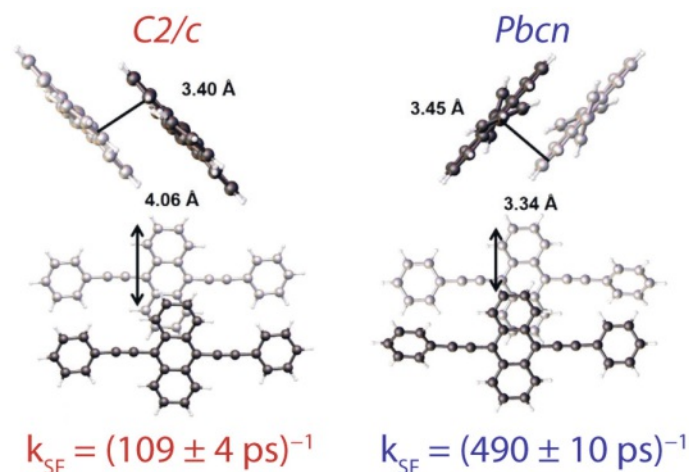

Fig. 5. a) Representative molecular dimers from the *C2/c* and *Pbcn* polymorphs of BPEA. The slip stacking and intermolecular distances as well as the resulting rate of singlet fission k$_{SF}$ are included for comparison. Adapted with permission from ref. [124]. Copyright 2018 American Chemical Society.

3.2 *SF in Aggregates*

While aggregation undoubtedly will impact the SF kinetics, SF (or TTA) in extended aggregates has, to date, not been studied in great detail. This may be in part due to the fact that conventional H- or J-aggregates are not formed by many of the conventional SF materials, rather these commonly form multidimensional HJ- or I-aggregates due to their herringbone arrangement.[106,107]

Nakano *et al.* have developed a theoretical framework to calculate SF rates in pentacene aggregate models with different configurations.[125–127] In particular, the model predicts that the SF rate of ring-shaped J-aggregates will monotonically decrease with increasing monomer number N. Ring-shaped H-aggregates on the other hand can show either an increase or a decrease in SF rate, with a maximal SF rate for N = 5.[126] In linear J-aggregates, the SF rate initially increases as N is increased up to N = 8. However, beyond N = 8, a decrease in the SF yield is predicted by the model, and for N > 12, the SF rate plateaus and remains constant. Further expanding the computational capabilities will without doubt facilitate the prediction of SF in aggregate structures.

Musser *et al.* reports the experimental investigation of SF in carotenoid aggregates with H- and J-type coupling.[62] For this, five different astaxanthin aggregates are formed *via* self-assembly and the SF dynamics are investigated. All aggregates generate triplet states on an ultrafast timescale – within the first picosecond, despite substantial differences in the lowest energy absorption band. The results indicate that the rate of triplet generation and subsequent annihilation is directly proportional to the intermolecular coupling strength. In contrast to the relaxation process on the molecular level which involves internal conversion to the 1A$_g$ state, the authors find no relevant intermediate states in the SF

process of the aggregates. The photoexcited $1B_u$ state undergoes SF directly, without internal conversion to $1A_g$.[62] This indicates that aggregation can result in additional relaxation pathways that are not present in the monomer itself.

4. Intermolecular Coupling in TTA-UC

While the effects of intermolecular coupling, crystal structure and symmetry are considerably well investigated for several SF materials, the same cannot be said for TTA-UC applications. While sensitized TTA-UC was introduced by Castellano[23,24,83] in the early 2000s, the majority of work since has been on solution-phase UC, where high UC quantum yields have been reported.[81,82,84,128] UC in polymer matrices,[27,86] organogels[87,89] and in solid-state have followed,[30,43,45,91] however, with limited success as discussed in detail by Alves et al.[5]

One of the major reasons why the same attention to detail of the TTA-UC process is not to be found in literature is the fact that there are a limited number of annihilators that have been successfully utilized in solid state. 9,10-diphenylanthracene is the 'drosophila' of annihilators used in solution due to its high quantum yields. However, the same success has not been demonstrated in solid state, in part, due to excimer formation.[129] On the other hand, the most commonly used triplet annihilator for solid-state thin film bilayer TTA-UC has been rubrene doped with dibenzo-tetraphenylperiflanthene (DBP) to mitigate the reverse process of SF.[28,75]

To first approximation the design principles of a successful SF system can be reverse engineered to fabricate a TTA-UC system. A singlet level $E(S_1) < 2 \times E(T_1)$ for exothermic TTA is the most important criterion, while strong electronic coupling is of lesser importance for successful TTA. However, the intermolecular coupling strength can be leveraged to alter the equilibrium between the competing processes of SF and TTA in systems capable of both.

Hence, if SF is more susceptible to changes in intermolecular coupling than TTA, this provides a means to move the equilibrium to UC. However, an additional factor plays a role in TTA-UC: the spin statistical factor η, which describes the probability that the encounter of two triplet states yields a singlet state. In the following, the impact of each of these factors on the UC yield is discussed.

4.1 Molecular Orientation vs. Spin Statistical Factor

The encounter of two triplet states can result in nine spin complexes: one spin singlet, three spin-triplet states and five quintet states.[56] Hence, η = 1/9 has been often assumed, yet experimentally determined values far exceed this value. Considering that quintet complexes easily dissociate back into the component triplet states, essentially recycling the triplet states and that triplet complexes result in the loss of a single triplet state, an overall theoretical value of η = 0.4 can be obtained in the strongly coupled limit.

However, spin statistical factors above 0.4 have been reported based on experimental observations. To understand the subtleties underlying the spin statistical factor, Bossanyi et al. investigated the role of the chromophore orientation and high level reverse intersystem crossing on the spin statistical factor.[130] Their results indicate that in the weakly exchange-coupled limit the molecular orientation can tune the spin statistical factor by spin mixing of the triplet-pair wave functions: 2/3 > η > 2/5 when going between parallel and perpendicular orientations, respectively.[130] Hence, the effect of the molecular orientation on η must be considered when designing a TTA-UC system.

4.2 Reducing SF to Increase TTA-UC

As previously mentioned, rubrene is capable of both SF and TTA since its singlet energy is nearly isoenergetic with twice the triplet energy. To demonstrate the important role of intermolecular coupling on the efficiency of TTA in competition with SF, bulky side groups can be added to shift the equilibrium between the two processes.

Bulky side groups have been shown to reduce the intermolecular coupling. Hence, they can reduce the efficiency of SF,[131] but also impact triplet diffusion in a thin film which can lead to reduced TTA. However, several reports have successfully demonstrated significant benefits of adding tert-butyl side groups to rubrene on the TTA-UC yield of rubrene.[132–134]

A detailed investigation by Baronas et al. investigated the impact of bulky tert-butyl side groups on TTA in rubrene.[132] For this, the properties of rubrene are compared to those of tetra(t-butyl)rubrene. The addition of the t-butyl groups results in a change of the crystal structure from orthorhombic to monoclinic, with a concurrent reduction in the spatial overlap of the π-electron systems as well as an increase in intermolecular spacing from 7.160 Å to 10.614 Å along the b-axis. In addition, the tetracene backbone π-π spacing increases from 3.7 Å for rubrene to 6.9 Å for tetra(t-butyl)rubrene.[132] The increased intermolecular spacing and changed molecular packing results in a decrease in SF, with a lesser impact on TTA.

4.3 Effect of Aggregation on TTA-UC

Moving beyond rubrene, Sullivan et al. have introduced several additional annihilators including 1-chloro-9,10-bis(phenylethynyl)anthracene (1-CBPEA) and naphtho[2,3-a]pyrene (NaPy) to increase the apparent anti-Stokes shift or energy gain during UC.[91,92] Interestingly, in contrast to rubrene which shows no sign of aggregation, both of these molecules exhibit an additional redshifted absorption feature in the solid state, indicating the presence of J-type coupling between individual molecules (Fig. 6a).
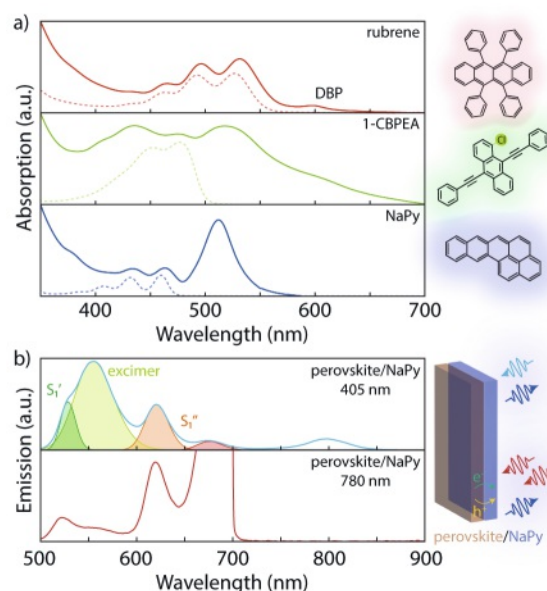

Fig. 6. a) Solid-state (solid lines) and solution (dashed lines) absorption spectra for rubrene, 1-chloro-9,10-bis(phenylethynyl)anthracene (1-CBPEA) and naphtho [2,3-a]pyrene (NaPy) highlighting the change in the spectral shape upon condensation into the solid state. b) Emission spectrum of a perovskite/NaPy bilayer under 405 nm (top) and 780 nm (bottom) excitation. Gaussian fits are included to highlight the different emissive states of NaPy: aggregate emission S_1', excimer emission and strongly coupled dimer emission S_1''. Data reproduced from refs. [90,91].

While aggregation can be detrimental to SF since the lowest energy singlet state is lowered in energy, possibly resulting in

endothermic SF, the opposite may be true for TTA-UC. Lowering of the singlet state energy may result in otherwise non TTA-active molecules to fulfil the energetic requirement for exothermic TTA: $E(S_1) < 2 \times E(T_1)$. Hence, this may result in an opportunity to tune the energetic landscape in favor of successful TTA for otherwise non TTA-active molecules.

Sullivan *et al*. report an interesting observation in NaPy: the emission spectrum obtained under direct excitation and during TTA-UC is not the same.[92] The emission spectrum consists of several distinct features: a rapidly decaying high energy aggregate-related feature centered at 520 nm (named S_1'), an excimer feature at 560 nm, and a much longer lived lower energy emissive feature (referred to as S_1'') at 620 nm with a corresponding vibronic progression, which was attributed to a localized J-coupled dimer.[135] The high energy feature dominates the emission spectrum when the molecule is excited directly, however, the lower energy feature dominates the UC emission spectrum (Fig. 6b).

Considering that the branching ratio between two emissive states should be the same, independent of the pathway through which the initial singlet state is excited, another underlying cause must be present to explain this observation. Several possible explanations exist: the true S_1 state is not achieved through TTA, energetically favorable conversion of the $^1(TT)$ state to the lower energy S_1'' state,[92] preferential TTA-UC at the lower energy sites, or increased SF at the higher energy S_1' states.

While the underlying cause is still subject to determination, it is clear that TTA-UC in the solid state is not a straightforward process – the impact of intermolecular interactions cannot be overlooked.

4. Conclusions

Predicting the optoelectronic properties of a molecule in condensed form is a quite difficult task; even for theoretical predictions, the crystal structure must be known. The molecular orientation in the crystal structure, transition dipole moment and intermolecular spacing play a key role in the intermolecular coupling strength.

Clearly, there is no 'one size fits all' approach to understanding or predicting SF and TTA in extended solid-state structures. The most important design parameter for efficient SF or TTA materials is an exothermic process. However, entropy can overcome small energy barriers for TTA/SF.[136,137] Intermolecular interactions can tune the lowest energy state, which will directly impact the energetic driving force for SF or TTA, possibly resulting in energetically unfavorable SF or TTA. However, decreased coupling commonly impacts SF rates to a greater extent than TTA rates, hence, molecular arrangement can be harnessed to shift the equilibrium of the reverse processes. However, reduced intermolecular coupling or crystalline disorder can impact the triplet diffusion rate, which in turn will impact the yield of TTA. However, the implication of aggregation on TTA-UC indicates that the singlet and triplet energies in solution phase are irrelevant – the relative energies in the condensed phase should be considered, which may lead to annihilators that are only TTA-active upon aggregation.

In summary, the local molecular arrangement is the key factor dictating the intermolecular dipole coupling, the exchange coupling required for SF/TTA, the spin statistical factor underlying TTA, as well as the prerequisite triplet diffusion. Additional studies will be required to gain a holistic understanding of the role of molecular arrangement on the rates of SF and TTA-UC.

[1] M. Einzinger, T. Wu, J. F. Kompalla, H. L. Smith, C. F. Perkinson, L. Nienhaus, S. Wieghold, D. N. Congreve, A. Kahn, M. G. Bawendi, M. A. Baldo, *Nature* **2019**, *571*, 90, https://doi.org/10.1038/s41586-019-1339-4.

[2] D. L. Dexter, *J. Lumin*. **1979**, *18–19*, 779, https://doi.org/10.1016/0022-2313(79)90235-7.

[3] I. Breen, R. Tempelaar, L. A. Bizimana, B. Kloss, D. R. Reichman, D. B. Turner, *J. Am. Chem. Soc*. **2017**, *139*, 11745, https://doi.org/10.1021/jacs.7b02621.

[4] M. Charbr, D. F. Williams, *Chem. Phys. Lett*. **1977**, *49*, 599, https://doi.org/10.1016/0009-2614(77)87048-6.

[5] J. Alves, J. Feng, L. Nienhaus, T. W. Schmidt, *J. Mater. Chem. C* **2022**, *10*, 7783, https://doi.org/10.1039/D1TC05659J.

[6] A. J. Carrod, V. Gray, K. Börjesson, *Energy Environ. Sci*. **2022**, *15*, 4982, https://doi.org/10.1039/D2EE01600A.

[7] B. S. Richards, D. Hudry, D. Busko, A. Turshatov, I. A. Howard, *Chem. Rev*. **2021**, *121*, 9165, https://doi.org/10.1021/acs.chemrev.1c00034.

[8] B. D. Ravetz, A. B. Pun, E. M. Churchill, D. N. Congreve, T. Rovis, L. M. Campos, *Nature* **2019**, *565*, 343, https://doi.org/10.1038/s41586-018-0835-2.

[9] J. Xu, P. Yang, M. Sun, H. Bi, B. Liu, D. Yang, S. Gai, F. He, J. Lin, *ACS Nano*. **2017**, *11*, 4133, https://doi.org/10.1021/acsnano.7b00944.

[10] M. You, J. Zhong, Y. Hong, Z. Duan, M. Lin, F. Xu, *Nanoscale* **2015**, *7*, 4423, https://doi.org/10.1039/C4NR06944G.

[11] S. Singh, W. J. Jones, W. Siebrand, B. P. Stoicheff, W. G. Schneider, *J. Chem. Phys*. **1965**, *42*, 330, https://doi.org/10.1063/1.1695695.

[12] G. B. Piland, J. J. Burdett, D. Kurunthu, C. J. Bardeen, *J. Phys. Chem. C* **2013**, *117*, 1224, https://doi.org/10.1021/jp309286v.

[13] T. Yago, K. Ishikawa, R. Katoh, M. Wakasa, *J. Phys. Chem. C* **2016**, *120*, 27858, https://doi.org/10.1021/acs.jpcc.6b09570.

[14] I. Papadopoulos, J. Zirzlmeier, C. Hetzer, Y. J. Bae, M. D. Krzyaniak, M. R. Wasielewski, T. Clark, R. R. Tykwinski, D. M. Guldi, *J. Am. Chem. Soc*. **2019**, *141*, 6191, https://doi.org/10.1021/jacs.8b09510.

[15] C. F. Perkinson, M. Einzinger, J. Finley, M. G. Bawendi, M. A. Baldo, *Adv. Materials* **2022**, *34*, 2103870, https://doi.org/10.1002/adma.202103870.

[16] T. Ullrich, D. Munz, D. M. Guldi, *Chem. Soc. Rev*. **2021**, *50*, 3485, https://doi.org/10.1039/D0CS01433H.

[17] Y. Y. Cheng, B. Fückel, R. W. MacQueen, T. Khoury, R. G. C. R. Clady, T. F. Schulze, N. J. Ekins-Daukes, M. J. Crossley, B. Stannowski, K. Lips, T. W. Schmidt, *Energy Environ. Sci*. **2012**, *5*, 6953, https://doi.org/10.1039/C2EE21136J.

[18] T. F. Schulze, J. Czolk, Y.-Y. Cheng, B. Fückel, R. W. MacQueen, T. Khoury, M. J. Crossley, B. Stannowski, K. Lips, U. Lemmer, A. Colsmann, T. W. Schmidt, *J. Phys. Chem. C* **2012**, *116*, 22794, https://doi.org/10.1021/jp309636m.

[19] R. W. MacQueen, M. Liebhaber, J. Niederhausen, M. Mews, C. Gersmann, S. Jäckle, K. Jäger, M. J. Y. Tayebjee, T. W. Schmidt, B. Rech, K. Lips, *Mater. Horiz*. **2018**, *5*, 1065, https://doi.org/10.1039/C8MH00853A.

[20] B. Daiber, S. Maiti, S. M. Ferro, J. Bodin, A. F. J. van den Boom, S. L. Luxembourg, S. Kinge, S. P. Pujari, H. Zuilhof, L. D. A. Siebbeles, B. Ehrler, *J. Phys. Chem. Lett*. **2020**, *11*, 8703, https://doi.org/10.1021/acs.jpclett.0c02163.

[21] N. J. Thompson, M. W. B. Wilson, D. N. Congreve, P. R. Brown, J. M. Scherer, T. S. Bischof, M. Wu, N. Geva, M. Welborn, T. V. Voorhis, V. Bulović, M. G. Bawendi, M. A. Baldo, *Nat. Mater*. **2014**, *13*, 1039, https://doi.org/10.1038/nmat4097.

[22] C. A. Parker, C. G. Hatchard, E. J. Bowen, *Proc. R. Soc. Lond. Ser. A. Math. Phys. Sci*. **1962**, *269*, 574, https://doi.org/10.1098/rspa.1962.0197.

[23] D. V. Kozlov, F. N. Castellano, *Chem. Commun*. **2004**, 2860, https://doi.org/10.1039/B412681E.

[24] W. Zhao, F. N. Castellano, *J. Phys. Chem. A* **2006**, *110*, 11440, https://doi.org/10.1021/jp064261s.

[25] R. R. Islangulov, F. N. Castellano, *Angew. Chem. Int. Ed*. **2006**, *45*, 5957, https://doi.org/10.1002/anie.200601615.

[26] T. N. Singh-Rachford, F. N. Castellano, *Coord. Chem. Rev*. **2010**, *254*, 2560, https://doi.org/10.1016/j.ccr.2010.01.003.

[27] R. R. Islangulov, J. Lott, C. Weder, F. N. Castellano, *J. Am. Chem. Soc*. **2007**, *129*, 12652, https://doi.org/10.1021/ja075014k.

[28] D. G. Bossanyi, Y. Sasaki, S. Wang, D. Chekulaev, N. Kimizuka, N. Yanai, J. Clark, *J. Mater. Chem. C* **2022**, *10*, 4684 https://doi.org/10.1039/D1TC02955J.

[29] X. Ma, F. Pan, H. Li, P. Shen, C. Ma, L. Zhang, H. Niu, Y. Zhu, S. Xu, H. Ye, *J. Phys. Chem. Lett*. **2019**, *10*, 5989, https://doi.org/10.1021/acs.jpclett.9b02289.

[30] L. Nienhaus, M. Wu, N. Geva, J. J. Shepherd, M. W. B. Wilson, V. Bulović, T. Van Voorhis, M. A. Baldo, M. G. Bawendi, *ACS Nano*. **2017**, *11*, 7848, https://doi.org/10.1021/acsnano.7b02024.

[31] S. Wieghold, A. S. Bieber, Z. A. VanOrman, L. Daley, M. Leger, J.-P. Correa-Baena, L. Nienhaus, *Matter* **2019**, *1*, 705, https://doi.org/10.1016/j.matt.2019.05.026.

[32] M. Mahboub, Z. Huang, M. L. Tang, *Nano. Letters* **2016**, *16*, 7169, https://doi.org/10.1021/acs.nanolett.6b03503.

[33] C. R. Conti, A. S. Bieber, Z. A. VanOrman, G. Moller, S. Wieghold, R. D. Schaller, G. F. Strouse, L. Nienhaus, *ACS Energy Lett.* **2022**, *7*, 617, https://doi.org/10.1021/acsenergylett.1c02732.

[34] C. M. Sullivan, A. S. Bieber, H. K. Drozdick, G. Moller, J. E. Kuszynski, Z. A. VanOrman, S. Wieghold, G. F. Strouse, L. Nienhaus, *Adv. Opt. Materials* **2023**, *11*, 2201921, https://doi.org/10.1002/adom.202201921.

[35] A. Monguzzi, R. Tubino, F. Meinardi, *J. Phys. Chem. A* **2009**, *113*, 1171, https://doi.org/10.1021/jp809971u.

[36] A. Ronchi, A. Monguzzi, *J. App. Phys.* **2021**, *129*, 050901, https://doi.org/10.1063/5.0034943.

[37] X. Luo, Y. Han, Z. Chen, Y. Li, G. Liang, X. Liu, T. Ding, C. Nie, M. Wang, F. N. Castellano, K. Wu, *Nature Commun.* **2020**, *11*, 28, https://doi.org/10.1038/s41467-019-13951-3.

[38] Y. Han, S. He, X. Luo, Y. Li, Z. Chen, W. Kang, X. Wang, K. Wu, *J. Am. Chem. Soc.* **2019**, *141*, 13033, https://doi.org/10.1021/jacs.9b07033.

[39] P. Xia, E. K. Raulerson, D. Coleman, C. S. Gerke, L. Mangolini, M. L. Tang, S. T. Roberts, *Nat. Chem.* **2020**, *12*, 137, https://doi.org/10.1038/s41557-019-0385-8.

[40] J. A. Bender, E. K. Raulerson, X. Li, T. Goldzak, P. Xia, T. Van Voorhis, M. L. Tang, S. T. Roberts, *J. Am. Chem. Soc.* **2018**, *140*, 7543, https://doi.org/10.1021/jacs.8b01966.

[41] G. D. Scholes, G. Rumbles, *Nat. Mater.* **2006**, *5*, 683, https://doi.org/10.1038/nmat1710.

[42] Z. Huang, Z. Xu, M. Mahboub, X. Li, J. W. Taylor, W. H. Harman, T. Lian, M. L. Tang, *Angew. Chem. Int. Ed.* **2017**, *129*, 16810, https://doi.org/10.1002/ange.201710224.

[43] L. Nienhaus, J.-P. Correa-Baena, S. Wieghold, M. Einzinger, T.-A. Lin, K. E. Shulenberger, N. D. Klein, M. Wu, V. Bulović, T. Buonassisi, M. A. Baldo, M. G. Bawendi, *ACS Energy Lett.* **2019**, *4*, 888, https://doi.org/10.1021/acsenergylett.9b00283.

[44] S. Wieghold, A. S. Bieber, Z. A. VanOrman, L. Nienhaus, *J. Phys. Chem. Lett.* **2019**, *10,* 3806, https://doi.org/10.1021/acs.jpclett.9b01526.

[45] K. Prashanthan, B. Naydenov, K. Lips, E. Unger, R. W. MacQueen, *J. Chem. Phys.* **2020**, *153*, 164711, https://doi.org/10.1063/5.0026564.

[46] M. B. Smith, J. Michl, *Chem. Rev.* **2010**, *110*, 6891, https://doi.org/10.1021/cr1002613.

[47] Z. A. VanOrman, H. K. Drozdick, S. Wieghold, L. Nienhaus, *J. Mater. Chem. C* **2021**, *9*, 2685, https://doi.org/10.1039/D1TC00245G.

[48] S. Wieghold, Z. A. VanOrman, L. Nienhaus, *Adv. Opt. Mater.* **2021**, *9*, 2001470, https://doi.org/10.1002/adom.202001470.

[49] M. B. Smith, J. Michl, *Ann. Rev. Phys. Chem.* **2013**, *64*, 361, https://doi.org/https://doi.org/10.1146/annurev-physchem-040412-110130.

[50] C. M. Sullivan, L. Nienhaus, *CHIMIA* **2024**, *78*, 518, https://doi.org/10.2533/chimia.2024.518.

[51] K. Miyata, F. S. Conrad-Burton, F. L. Geyer, X.-Y. Zhu, *Chem. Rev.* **2019**, *119*, 4261, https://doi.org/10.1021/acs.chemrev.8b00572.

[52] M. J. Y. Tayebjee, S. N. Sanders, E. Kumarasamy, L. M. Campos, M. Y. Sfeir, D. R. McCamey, *Nat. Phys.* **2017**, *13*, 182, https://doi.org/10.1038/nphys3909.

[53] H. Nagashima, S. Kawaoka, S. Akimoto, T. Tachikawa, Y. Matsui, H. Ikeda, Y. Kobori, *J. Phys. Chem. Lett.* **2018**, *9*, 5855, https://doi.org/10.1021/acs.jpclett.8b02396.

[54] K. E. Smyser, J. D. Eaves, *Sci. Rep.* **2020**, *10*, 18480, https://doi.org/10.1038/s41598-020-75459-x.

[55] N. A. Pace, B. K. Rugg, C. H. Chang, O. G. Reid, K. J. Thorley, S. Parkin, J. E. Anthony, J. C. Johnson, *Chem. Sci.* **2020**, *11*, 7226, https://doi.org/10.1039/D0SC02497J.

[56] R. E. Merrifield, *Pure Appl. Chem.* **1971**, *27*, 481, https://doi.org/10.1351/pac197127030481.

[57] A. M. Müller, Y. S. Avlasevich, W. W. Schoeller, K. Müllen, C. J. Bardeen, *J. Am. Chem. Soc.* **2007**, *129*, 14240, https://doi.org/10.1021/ja073173y.

[58] G. B. Piland, C. J. Bardeen, *J. Phys. Chem. Lett.* **2015**, *6*, 1841, https://doi.org/10.1021/acs.jpclett.5b00569.

[59] R. E. Merrifield, P. Avakian, R. P. Groff, *Chem. Phys. Lett.* **1969**, *3*, 155, https://doi.org/10.1016/0009-2614(69)80122-3.

[60] S. Paul, V. Karunakaran, *J. Phys. Chem. B* **2022**, *126*, 1054, https://doi.org/10.1021/acs.jpcb.1c07951.

[61] C. Wang, M. J. Tauber, *J. Am. Chem. Soc.* **2010**, *132*, 13988, https://doi.org/10.1021/ja102851m.

[62] A. J. Musser, M. Maiuri, D. Brida, G. Cerullo, R. H. Friend, J. Clark, *J. Am. Chem. Soc.* **2015**, *137*, 5130, https://doi.org/10.1021/jacs.5b01130.

[63] G. Lanzani, S. Stagira, G. Cerullo, S. De Silvestri, D. Comoretto, I. Moggio, C. Cuniberti, G. F. Musso, G. Dellepiane, *Chem. Phys. Lett.* **1999**, *313*, 525, https://doi.org/10.1016/S0009-2614(99)01104-5.

[64] J. Guo, H. Ohkita, H. Benten, S. Ito, *J. Am. Chem. Soc.* **2009**, *131*, 16869, https://doi.org/10.1021/ja906621a.

[65] M. Dvořák, S. K. K. Prasad, C. B. Dover, C. R. Forest, A. Kaleem, R. W. MacQueen, A. J. I. Petty, R. Forecast, J. E. Beves, J. E. Anthony, M. J. Y. Tayebjee, A. Widmer-Cooper, P. Thordarson, T. W. Schmidt, *J. Am. Chem. Soc.* **2021**, *143*, 13749, https://doi.org/10.1021/jacs.1c05767.

[66] Y. J. Bae, G. Kang, C. D. Malliakas, J. N. Nelson, J. Zhou, R. M. Young, Y.-L. Wu, R. P. Van Duyne, G. C. Schatz, M. R. Wasielewski, *J. Am. Chem. Soc.* **2018**, *140*, 15140, https://doi.org/10.1021/jacs.8b07498.

[67] C. Grieco, G. S. Doucette, K. T. Munson, J. R. Swartzfager, J. M. Munro, J. E. Anthony, I. Dabo, J. B. Asbury, *J. Chem. Phys.* **2019**, *151*, 154701, https://doi.org/10.1063/1.5116586.

[68] B. J. Walker, A. J. Musser, D. Beljonne, R. H. Friend, *Nat. Chem.* **2013**, *5*, 1019, https://doi.org/10.1038/nchem.1801.

[69] H.-J. Jang, E. G. Bittle, Q. Zhang, A. J. Biacchi, C. A. Richter, D. J. Gundlach, *ACS Nano.* **2019**, *13*, 616, https://doi.org/10.1021/acsnano.8b07625.

[70] J. J. Burdett, C. J. Bardeen, *Acc. Chem. Res.* **2013**, *46*, 1312, https://doi.org/10.1021/ar300191w.

[71] P. E. Teichen, J. D. Eaves, *J. Chem. Phys.* **2015**, *143*, 044118, https://doi.org/10.1063/1.4922644.

[72] K. T. Munson, J. Gan, C. Grieco, G. S. Doucette, J. E. Anthony, J. B. Asbury, *J. Phys. Chem. C* **2020**, *124*, 23567, https://doi.org/10.1021/acs.jpcc.0c07920.

[73] S. T. Roberts, R. E. McAnally, J. N. Mastron, D. H. Webber, M. T. Whited, R. L. Brutchey, M. E. Thompson, S. E. Bradforth, *J. Am. Chem. Soc.* **2012**, *134*, 6388, https://doi.org/10.1021/ja300504t.

[74] D. M. Finton, E. A. Wolf, V. S. Zoutenbier, K. A. Ward, I. Biaggio, *AIP Adv.* **2019**, *9*, 095027, https://doi.org/10.1063/1.5118942.

[75] S. Wieghold, A. S. Bieber, Z. A. VanOrman, A. Rodriguez, L. Nienhaus, *J. Phys. Chem. C* **2020**, *124*, 18132, https://doi.org/10.1021/acs.jpcc.0c05290.

[76] J. J. Burdett, C. J. Bardeen, *Acc. Chem. Res.* **2013**, *46*, 1312, https://doi.org/10.1021/ar300191w.

[77] N. V. Korovina, S. Das, Z. Nett, X. Feng, J. Joy, R. Haiges, A. I. Krylov, S. E. Bradforth, M. E. Thompson, *J. Am. Chem. Soc.* **2016**, *138*, 617, https://doi.org/10.1021/jacs.5b10550.

[78] N. V. Korovina, J. Joy, X. Feng, C. Feltenberger, A. I. Krylov, S. E. Bradforth, M. E. Thompson, *J. Am. Chem. Soc.* **2018**, *140*, 10179, https://doi.org/10.1021/jacs.8b04401.

[79] B. S. Basel, J. Zirzlmeier, C. Hetzer, S. R. Reddy, B. T. Phelan, M. D. Krzyaniak, M. K. Volland, P. B. Coto, R. M. Young, T. Clark, M. Thoss, R. R. Tykwinski, M. R. Wasielewski, D. M. Guldi, *Chem* **2018**, *4*, 1092, https://doi.org/10.1016/j.chempr.2018.04.006.

[80] S. N. Sanders, E. Kumarasamy, K. J. Fallon, M. Y. Sfeir, L. M. Campos, *Chem. Sci.* **2020**, *11*, 1079, https://doi.org/10.1039/C9SC05066C.

[81] S. Amemori, Y. Sasaki, N. Yanai, N. Kimizuka, *J. Am. Chem. Soc.* **2016**, *138*, 8702, https://doi.org/10.1021/jacs.6b04692.

[82] K. Mase, K. Okumura, N. Yanai, N. Kimizuka, *Chem. Commun.* **2017**, *53*, 8261, https://doi.org/10.1039/C7CC03087H.

[83] T. N. Singh-Rachford, F. N. Castellano, *J. Phys. Chem. A* **2008**, *112*, 3550, https://doi.org/10.1021/jp7111878.

[84] Z. A. VanOrman, A. S. Bieber, S. Wieghold, L. Nienhaus, *Chem. Mater.* **2020**, *32*, 4734, https://doi.org/10.1021/acs.chemmater.0c01354.

[85] Z. A. VanOrman, C. R. Conti, G. F. Strouse, L. Nienhaus, *Chem. Mater.* **2021**, *33*, 452, https://doi.org/10.1021/acs.chemmater.0c04468.

[86] F. Saenz, A. Ronchi, M. Mauri, R. Vadrucci, F. Meinardi, A. Monguzzi, C. Weder, *Adv. Func. Mat.* **2021**, *31*, 2004495, https://doi.org/10.1002/adfm.202004495.

[87] R. Vadrucci, C. Weder, Y. C. Simon, *Mater. Horiz.* **2015**, *2*, 120, https://doi.org/10.1039/C4MH00168K.

[88] R. O'Shea, C. Gao, T. C. Owyong, J. M. White, W. W. H. Wong, *Mater. Adv.* **2021**, *2*, 2031, https://doi.org/10.1039/D1MA00068C.

[89] K. Sripathy, R. W. MacQueen, J. R. Peterson, Y. Y. Cheng, M. Dvořák, D. R. McCamey, N. D. Treat, N. Stingelin, T. W. Schmidt, *J. Mater. Chem. C* **2015**, *3*, 616, https://doi.org/10.1039/C4TC02584A.

[90] N. Geva, L. Nienhaus, M. Wu, V. Bulović, M. A. Baldo, T. Van Voorhis, M. G. Bawendi, *J. Phys. Chem. Lett.* **2019**, *10*, 3147, https://doi.org/10.1021/acs.jpclett.9b01058.

[91] C. M. Sullivan, L. Nienhaus, *Nanoscale* **2022**, *14*, 17254, https://doi.org/10.1039/D2NR05309H.

[92] C. M. Sullivan, L. Nienhaus, *Chem. Mater.* **2024**, *36*, 417, https://doi.org/10.1021/acs.chemmater.3c02349.

[93] N. J. Hestand, F. C. Spano, *Chem. Rev.* **2018**, *118*, 7069, https://doi.org/10.1021/acs.chemrev.7b00581.

[94] J. L. Charlton, R. Dabestani, J. Saltiel, *J. Am. Chem. Soc.* **1983**, *105*, 3473, https://doi.org/10.1021/ja00349a017.

[95] T. Schillmöller, R. Herbst-Irmer, D. Stalke, *Adv. Opt. Mater.* **2021**, *9*, 2001814, https://doi.org/10.1002/adom.202001814.

[96] J. K. McVey, D. M. Shold, N. C. Yang, *J. Chem. Phys.* **1976**, *65*, 3375, https://doi.org/10.1063/1.433468.

[97] A. Nandi, B. Manna, R. Ghosh, *Phys. Chem. Chem. Phys.* **2019**, *21*, 11193, https://doi.org/10.1039/C9CP01124B.

[98] B. Manna, A. Nandi, S. Nath, N. Agarwal, R. Ghosh, *J. Photochem. Photobio. A: Chem.* **2020**, *400*, 112700, https://doi.org/10.1016/j.jphotochem.2020.112700.

[99] J B Birks, *Rep. Prog. Phys.* **1975**, *38*, 903, https://doi.org/10.1088/0034-4885/38/8/001.

[100] F. C. Spano, C. Silva, *Annu. Rev. Phys. Chem.* **2014**, *65*, 477, https://doi.org/10.1146/annurev-physchem-040513-103639.

[101] S.-H. Lim, T. G. Bjorklund, F. C. Spano, C. J. Bardeen, *Phys. Rev. Lett.* **2004**, *92*, 107402, https://doi.org/10.1103/PhysRevLett.92.107402.

[102] E. G. McRae, M. Kasha, *J. Chem. Phys.* **1958**, *28*, 721, https://doi.org/10.1063/1.1744225.

[103] R. M. Hochstrasser, M. Kasha, *Photochem. Photobio.* **1964**, *3*, 317, https://doi.org/10.1111/j.1751-1097.1964.tb08155.x.

[104] M. Kasha, *Radiation Res.* **1963**, *20*, 55, https://doi.org/10.2307/3571331.

[105] E. E. Jelley, *Nature* **1936**, *138*, 1009, https://doi.org/10.1038/1381009a0.

[106] H. Yamagata, F. C. Spano, *J. Chem. Phys.* **2012**, *136*, 184901, https://doi.org/10.1063/1.4705272.

[107] A. P. Deshmukh, N. Geue, N. C. Bradbury, T. L. Atallah, C. Chuang, M. Pengshung, J. Cao, E. M. Sletten, D. Neuhauser, J. R. Caram, *Chem. Phys. Rev.* **2022**, *3*, 021401, https://doi.org/10.1063/5.0094451.

[108] A. P. Deshmukh, D. Koppel, C. Chuang, D. M. Cadena, J. Cao, J. R. Caram, *J. Phys. Chem. C* **2019**, *123*, 18702, https://doi.org/10.1021/acs.jpcc.9b05060.

[109] E. C. Greyson, B. R. Stepp, X. Chen, A. F. Schwerin, I. Paci, M. B. Smith, A. Akdag, J. C. Johnson, A. J. Nozik, J. Michl, M. A. Ratner, *J. Phys. Chem. B* **2010**, *114*, 14223, https://doi.org/10.1021/jp909002d.

[110] H. Zang, Y. Zhao, W. Liang, *J. Phys. Chem. Lett.* **2017**, *8*, 5105, https://doi.org/10.1021/acs.jpclett.7b01996.

[111] S. R. Yost, J. Lee, M. W. B. Wilson, T. Wu, D. P. McMahon, R. R. Parkhurst, N. J. Thompson, D. N. Congreve, A. Rao, K. Johnson, M. Y. Sfeir, M. G. Bawendi, T. M. Swager, R. H. Friend, M. A. Baldo, T. Van Voorhis, *Nat. Chem.* **2014**, *6*, 492, https://doi.org/10.1038/nchem.1945.

[112] R. A. Marcus, *Rev. Mod. Phys.* **1993**, *65*, 599, https://doi.org/10.1103/RevModPhys.65.599.

[113] R. A. Marcus, *J. Chem. Phys.* **1956**, *24*, 966, https://doi.org/10.1063/1.1742723.

[114] J. Jortner, M. Bixon, *J. Chem. Phys.* **1988**, *88*, 167, https://doi.org/10.1063/1.454632.

[115] S. Fan, W. Li, T. Li, F. Gao, W. Hu, S. Liu, X. Wang, H. Liu, Z. Liu, Z. Li, Y. Chen, X. Li, *J. Photochem. Photobiol. A: Chem.* **2022**, *427*, 113826, https://doi.org/10.1016/j.jphotochem.2022.113826.

[116] R. A. Marcus, *Rev. Mod. Phys.* **1993**, *65*, 599, https://doi.org/10.1103/RevModPhys.65.599.

[117] H. Marciniak, M. Fiebig, M. Huth, S. Schiefer, B. Nickel, F. Selmaier, S. Lochbrunner, *Phys. Rev. Lett.* **2007**, *99*, 176402, https://doi.org/10.1103/PhysRevLett.99.176402.

[118] J. Guo, H. Ohkita, H. Benten, S. Ito, *J. Am. Chem. Soc.* **2009**, *131*, 16869, https://doi.org/10.1021/ja906621a.

[119] M. Wu, D. N. Congreve, M. W. B. Wilson, J. Jean, N. Geva, M. Welborn, T. Van Voorhis, V. Bulović, M. G. Bawendi, M. A. Baldo, *Nat. Photonics* **2016**, *10*, 31, https://doi.org/10.1038/nphoton.2015.226.

[120] M. J. Y. Tayebjee, R. G. C. R. Clady, T. W. Schmidt, *Phys. Chem. Chem. Phys.* **2013**, *15*, 14797, https://doi.org/10.1039/C3CP52609G.

[121] W. Mou, S. Hattori, P. Rajak, F. Shimojo, A. Nakano, *App. Phys. Lett.* **2013**, *102*, 173301, https://doi.org/10.1063/1.4795138.

[122] T. S. Volek, Z. T. Armstrong, J. K. Sowa, K. S. Wilson, M. Bohlmann Kunz, K. Bera, M. Koble, R. R. Frontiera, P. J. Rossky, M. T. Zanni, S. T. Roberts, *J. Phys. Chem. Lett.* **2023**, *14*, 11497, https://doi.org/10.1021/acs.jpclett.3c02845.

[123] K. Miyata, Y. Kurashige, K. Watanabe, T. Sugimoto, S. Takahashi, S. Tanaka, J. Takeya, T. Yanai, Y. Matsumoto, *Nature Chem.* **2017**, *9*, 983, https://doi.org/10.1038/nchem.2784.

[124] R. D. Pensack, C. Grieco, G. E. Purdum, S. M. Mazza, A. J. Tilley, E. E. Ostroumov, D. S. Seferos, Y.-L. Loo, J. B. Asbury, J. E. Anthony, G. D. Scholes, *Mater. Horiz.* **2017**, *4*, 915, https://doi.org/10.1039/C7MH00303J.

[125] M. Nakano, *J. Chem. Phys.* **2019**, *150*, 234305, https://doi.org/10.1063/1.5100116.

[126] H. Miyamoto, M. Nakano, *ChemPhotoChem* **2020**, *4*, 5249, https://doi.org/10.1002/cptc.202000089.

[127] M. Nakano, T. Nagami, T. Tonami, K. Okada, S. Ito, R. Kishi, Y. Kitagawa, T. Kubo, *J. Comp. Chem.* **2019**, *40*, 89, https://doi.org/10.1002/jcc.25539.

[128] N. Harada, Y. Sasaki, M. Hosoyamada, N. Kimizuka, N. Yanai, *Angew. Chem. Int. Ed.* **2021**, *60*, 142, https://doi.org/10.1002/anie.202012419.

[129] A. Nandi, B. Manna, R. Ghosh, *Phys. Chem. Chem. Phys.* **2019**, *21*, 11193, https://doi.org/10.1039/C9CP01124B.

[130] D. G. Bossanyi, Y. Sasaki, S. Wang, D. Chekulaev, N. Kimizuka, N. Yanai, J. Clark, *JACS Au* **2021**, *1*, 2188, https://doi.org/10.1021/jacsau.1c00322.

[131] R. Nagata, H. Nakanotani, W. J. Potscavage Jr., C. Adachi, *Adv. Mater.* **2018**, *30*, 1801484, https://doi.org/10.1002/adma.201801484.

[132] P. Baronas, G. Kreiza, L. Naimovičius, E. Radiunas, K. Kazlauskas, E. Orentas, S. Juršėnas, *J. Phys. Chem. C* **2022**, *126*, 15327, https://doi.org/10.1021/acs.jpcc.2c04572.

[133] E. Radiunas, M. Dapkevičius, S. Raišys, S. Juršėnas, A. Jozeliūnaitė, T. Javorskis, U. Šinkevičiūtė, E. Orentas, K. Kazlauskas, *Phys. Chem. Chem. Phys.* **2020**, *22*, 7392, https://doi.org/10.1039/D0CP00144A.

[134] A. Sawa, S. Shimada, N. Tripathi, C. Heck, H. Tachibana, E. Koyama, T. Mizokuro, Y. Hirao, T. Kubo, N. Tamai, D. Kuzuhara, H. Yamada, K. Kamada, *J. Mater. Chem. C* **2023**, *11*, 8502, https://doi.org/10.1039/D3TC00853C.

[135] C. M. Sullivan, A. M. Szucs, T. Siegrist, L. Nienhaus, *J. Phys. Chem. C* **2024**, https://doi.org/10.1021/acs.jpcc.4c05675.

[136] W.-L. Chan, M. Ligges, X.-Y. Zhu, *Nat. Chem.* **2012**, *4*, 840, https://doi.org/10.1038/nchem.1436.

[137] Y. Y. Cheng, B. Fückel, T. Khoury, R. G. C. R. Clady, N. J. Ekins-Daukes, M. J. Crossley, T. W. Schmidt, *J. Phys. Chem. A* **2011**, *115*, 1047, https://doi.org/10.1021/jp108839g.